



# Thermal correction Judd-Ofelt analyze of $\text{Eu}^{3+}$ ion doped calcium gadolinium silicoborate oxyfluoride glass

Nuanthip WANTANA<sup>1,2</sup>, Yotsakit RUANGTAWEEP<sup>1,2,\*</sup>, and Jakrapong KAEWKHAO<sup>1,2</sup>

<sup>1</sup>Physics Program, Faculty of Science and Technology, Nakhon Pathom Rajabhat University, Nakhon Pathom, 73000, Thailand

<sup>2</sup>Center of Excellence in Glass Technology and Materials Science (CEGM), Nakhon Pathom Rajabhat University, Nakhon Pathom, 73000, Thailand

\*Corresponding author e-mail: yotsakitt@hotmail.com, Djone@npru.ac.th

## Received date:

4 June 2018

## Revised date:

3 July 2018

## Accepted date:

31 August 2018

## Keywords:

Oxyfluoride

Europium

Radiative parameter

Judd-Ofelt theory

## Abstract

The Calcium Gadolinium Silicoborate Oxyfluoride glass doped with 1.0 mol% of  $\text{Eu}^{3+}$  concentration. ( $\text{CaGdSiBF:Eu}^{3+}$ ) was prepared by a melt quenching technique for study in the absorption and emission properties. Glass absorbed photon in ultraviolet, visible light and near infrared regions. The excitation with 275 nm of  $\text{Gd}^{3+}$  show the strongest red emission at 613 nm from  ${}^5\text{D}_0 \rightarrow {}^7\text{F}_2$  transition. The Judd-Ofelt (J-O) intensity parameters are derived from the integrated area under absorption and emission, including the refractive index. The thermal correction was used to improve J-O analysis from an uncertainty of  $\text{Eu}^{3+}$  population on the ground state. The spectroscopic results were used to calculate the radiative parameter via J-O theory using a normal calculation method compared with a thermal-correction calculation method to analyze a potential in laser application. The color coordinates (x,y) under 275 nm excitation wavelength were (0.64, 0.36), that be plotted in the reddish orange region of CIE 1931 chromaticity diagram.  $\text{CaGdSiBF:Eu}^{3+}$  glass performs the high lasing power and energy extraction ratio, which can be developed for using as a laser medium in red laser device.

## 1. Introduction

In present, optical devices are used extensively in several activity of human. New light source devices have been always studied and developed to get a good performance. A good light emitting is gained from quite material, it was found that glass doped with lanthanide ion is now very interesting for optical devices development including solid-state lasers, fiber amplifiers, infrared to visible light up-converters, field emission displays, etc. [1-4]. Borate compound can form glass by itself using low melting point, obtained glass shows good transparency and high chemical durability [5]. Silicate glass is the most refractory glass in commercial use. It has a high chemical resistance, low electrical conductivity, low thermal expansion and good UV transparency [5]. Oxyfluoride glasses are very attractive because of their various application in photonics devices [6]. Fluorides are known as excellent hosts for RE ions due to low phonon energy, small band gap, high density, substantial thermal and mechanical strength [7,8]. Gadolinium oxide ( $\text{Gd}_2\text{O}_3$ ) has become a material

of attention within the glass matrix because of highly efficient energy transfer from the  $\text{Gd}^{3+}$  ions to the incorporated activators, at an available cost [2]. The choice of silicoborate network is based on the fact that the addition of CaO into silicoborate glasses improves the intensity of optical absorption and luminescence emission in glass [2,9]. Among the  $\text{RE}^{3+}$  ions,  $\text{Eu}^{3+}$  is unique ion because of the strong emission in red-orange region [1,3,10]. The intra-4f shell transitions are relatively well shielded from the surrounding ligand field making  $\text{Eu}^{3+}$  narrow luminescence line positions nearly independent of the host material [6]. Since the ground  ${}^7\text{F}_0$  state and the fluorescent  ${}^5\text{D}_0$  state of  $\text{Eu}^{3+}$  ions are non-degenerate under any symmetry, information regarding the local environment around the  $\text{Eu}^{3+}$  ion strongly depends only on the splitting of the  ${}^5\text{D}_0 \rightarrow {}^7\text{F}_{1,2}$  transitions in emission spectra [1,3]. It was performed for the  ${}^7\text{F}_0 \rightarrow {}^5\text{D}_0$  transition of  $\text{Eu}^{3+}$  ion at room temperature which has potential use in high-density optical data storage [4,11].

In this work, we prepared the  $\text{Eu}^{3+}$  doped calcium gadolinium silicoborate oxyfluoride glass and then investigated its spectroscopic properties. The J-O

analysis was used to determine this glass potential for using as laser gain medium.

## 2. Experimental

The  $\text{Eu}^{3+}$  doped calcium gadolinium silicoborate oxyfluoride ( $\text{CaGdSiBFEu}$ ) glass with compositions of  $10\text{CaF}-25\text{GdF}_3-10\text{SiO}_2-54\text{B}_2\text{O}_3-1\text{Eu}_2\text{O}_3$  was prepared by the melt quenching technique. The chemicals,  $\text{CaF}$ ,  $\text{GdF}_3$ ,  $\text{SiO}_2$ ,  $\text{H}_3\text{BO}_3$  and  $\text{Eu}_2\text{O}_3$  with high purity was totally weighted to 10 g and was mixed thoroughly in an alumina crucible and melted at  $1400^\circ\text{C}$  for 3 hours in an electric furnace. Glassy liquid was quenched in preheated stainless-steel molds. Obtained glass was annealed at  $500^\circ\text{C}$  for 3 hours in order to remove thermal strains and then cut and polished. The density of glass was measured by applying the Archimedes' principle, weighted sample in air and water via a 4-digit sensitive microbalance (AND, HR 200). The optical spectrum was measured with a UV-VIS-NIR spectrophotometer (Shimadzu UV-3600) in the range of ultraviolet, visible and near-infrared region. The excitation, emission spectrum and lifetime were collected by using a spectrofluorophotometer (Cary-Eclipse) with xenon lamp as a light source. The refractive index ( $n$ ), is measured by an Abbe refractometer which used light of  $589\text{ nm}$  and 1-Bromonaphthalin as contact liquid. The absorption spectrum, emission spectrum and refractive index were used to analyze lasing ability of glass via Judd-Ofelt (JO) theory [1] which contains spectroscopic interaction parameters such as oscillator strength ( $f$ ), JO intensity parameter ( $\Omega_\lambda$ ,  $\lambda = 2, 4, 6$ ), radiative transition probability ( $A_R$ ), stimulated emission cross-section ( $\sigma$ ) and branching ratio ( $\beta_R$ ). Optical band gaps was calculated for indirect and direct transitions from the absorption spectrum of glass [12,13]. The chemical bonds inside the glass matrix was investigated by Fourier-transform infrared (FTIR) spectrometer. CIE 1931 chromaticity diagram (the diagram that defined quantitative links between physical pure color in the electromagnetic visible spectrum and physiological perceived color in human color vision) was used to determine color of the emitted light obtained from the emission spectrum.

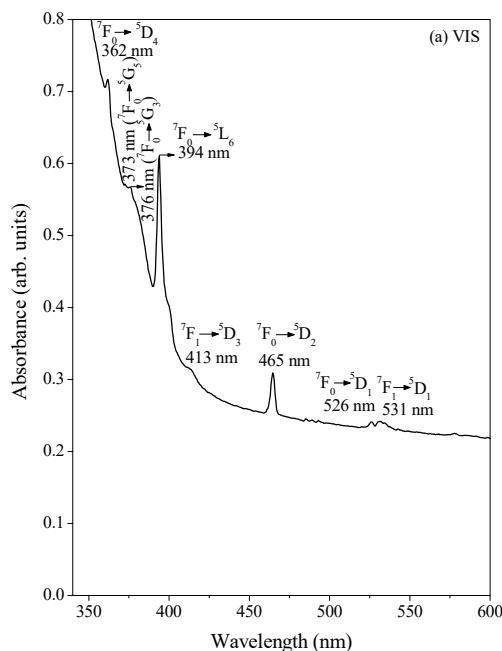


**Figure 1.** The absorption spectrum of the  $\text{CaGdSiBFEu}$  glass in VIS region.

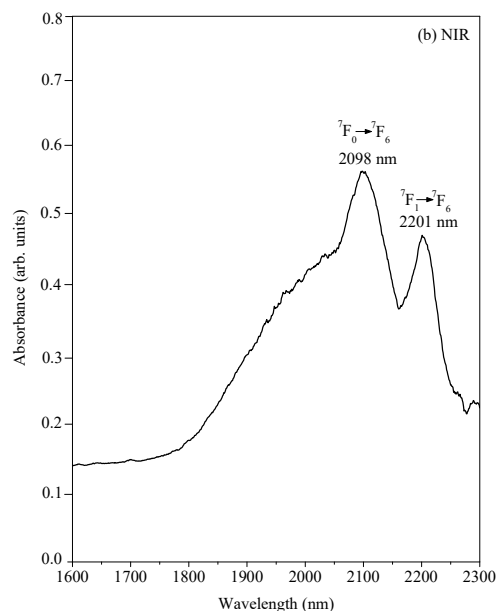


**Figure 2.** The absorption spectrum of the  $\text{CaGdSiBFEu}$  glass in NIR region.

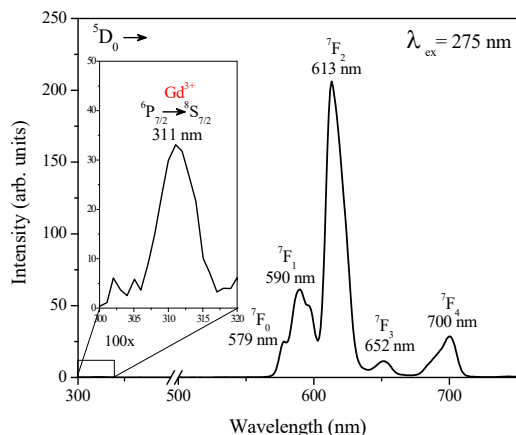


**Figure 3.** The emission spectrum of the CaGdSiBFEu glass.

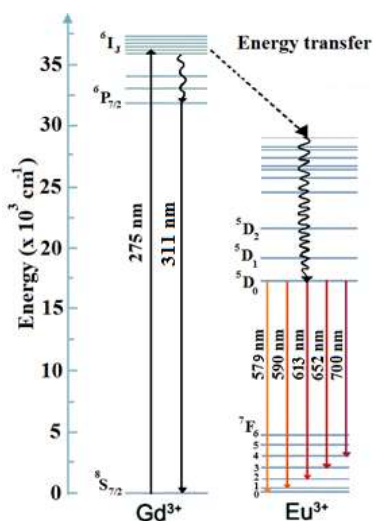


**Figure 4.** Energy level diagram of Gd<sup>3+</sup> and Eu<sup>3+</sup> ions in glass.

### 3. Results and discussion

The absorption spectrum of CaGdSiBFEu glass was recorded from visible light (VIS) to near infrared (NIR) region and shown in figure 1 and 2. The absorption spectrum contains ten absorption bands, 362, 373, 376, 394, 413, 465, 526, 531, 2098 and 2201 nm, which correspond to energy transitions of Eu<sup>3+</sup> from ground state (<sup>7</sup>F<sub>0</sub> or <sup>7</sup>F<sub>1</sub>) to excited states of <sup>7</sup>F<sub>0</sub>→<sup>5</sup>D<sub>4</sub>, <sup>7</sup>F<sub>0</sub>→<sup>5</sup>G<sub>5</sub>, <sup>7</sup>F<sub>0</sub>→<sup>5</sup>G<sub>3</sub>, <sup>7</sup>F<sub>0</sub>→<sup>5</sup>L<sub>6</sub>, <sup>7</sup>F<sub>0</sub>→<sup>5</sup>D<sub>3</sub>, <sup>7</sup>F<sub>0</sub>→<sup>5</sup>D<sub>2</sub>, <sup>7</sup>F<sub>0</sub>→<sup>5</sup>D<sub>1</sub>, <sup>7</sup>F<sub>1</sub>→<sup>5</sup>D<sub>1</sub>, <sup>7</sup>F<sub>0</sub>→<sup>7</sup>F<sub>6</sub> and <sup>7</sup>F<sub>1</sub>→<sup>7</sup>F<sub>6</sub>, respectively [1,3]. The emission spectrum of the CaGdSiBFEu glass under 275 nm of Gd<sup>3+</sup> excitation was recorded and shown in figure 3. It was found five emission bands at 579, 590, 613, 652 and 700 nm representing the energy

transitions of the Eu<sup>3+</sup> such as <sup>5</sup>D<sub>0</sub>→<sup>4</sup>F<sub>0</sub>, <sup>5</sup>D<sub>0</sub>→<sup>7</sup>F<sub>1</sub>, <sup>5</sup>D<sub>0</sub>→<sup>7</sup>F<sub>2</sub>, <sup>5</sup>D<sub>0</sub>→<sup>7</sup>F<sub>3</sub> and <sup>5</sup>D<sub>0</sub>→<sup>7</sup>F<sub>4</sub>, respectively [1,3]. The strongest band belongs to 613 nm wavelength (<sup>5</sup>D<sub>0</sub>→<sup>7</sup>F<sub>2</sub>). For inset picture in figure 3, it shows the enlargement of Gd<sup>3+</sup> emission band at 311 nm. All process of luminescence such as Gd<sup>3+</sup> excitation and emission, Gd<sup>3+</sup>-Eu<sup>3+</sup> energy transfer, non-radiative relaxation and Eu<sup>3+</sup> emission are shown in figure 4.

The J–O analysis to study potential of glass for laser medium applications. In the case of Eu<sup>3+</sup> ion, the absorption transitions starting not only from <sup>7</sup>F<sub>0</sub> state but also from <sup>7</sup>F<sub>1</sub> state can be observed and some of these transitions often overlap which makes J–O analysis [1,3] to be complicate at room temperature. Since, <sup>7</sup>F<sub>J</sub> (J = 0, 1 and 2) levels are populated thermally at room temperature, the fractional thermal populations of the <sup>7</sup>F<sub>0</sub>, <sup>7</sup>F<sub>1</sub> and <sup>7</sup>F<sub>2</sub> levels are calculated to be 59%, 38% and 3%, respectively. Therefore, the population of <sup>7</sup>F<sub>1</sub> level cannot be neglected at room temperature. The absorption spectrum and refractive index were used to analyse the lasing ability of glass via the J–O theory with and without correction from fractional thermal populations. As the absorption originates from the ground <sup>7</sup>F<sub>0</sub> as well as thermally populated <sup>7</sup>F<sub>1</sub> states, the oscillator strengths are corrected for thermalization effect at room temperature by dividing the respective population of <sup>7</sup>F<sub>0,1</sub> levels [1,3]. The experimental ( $f_{exp}$ ) and calculated ( $f_{cal}$ ) oscillator strengths of observed absorption levels and J–O parameters ( $\Omega_\lambda$ ) with and without thermal correction are presented in table 1. The  $f_{exp}$  and  $f_{cal}$  are close together representing the good fitting result. The oscillator strengths values of <sup>7</sup>F<sub>0</sub>→<sup>5</sup>L<sub>6</sub> (394 nm) and <sup>7</sup>F<sub>0</sub>→<sup>7</sup>F<sub>6</sub> (2098 nm) transition is higher more than others in VIS and NIR region, respectively which corresponds to the peak absorbance in spectrum. The J–O parameters obtained from without thermal correction are  $\Omega_2 = 10.41 \times 10^{-20} \text{ cm}^2$ ,  $\Omega_4 = 10.05 \times 10^{-20} \text{ cm}^2$  and  $\Omega_6 = 1.99 \times 10^{-20} \text{ cm}^2$ , while values obtained with thermal correction are  $\Omega_2 = 25.66 \times 10^{-20} \text{ cm}^2$ ,  $\Omega_4 = 20.34 \times 10^{-20} \text{ cm}^2$  and  $\Omega_6 = 4.70 \times 10^{-20}$ . The  $\Omega_2$  parameter often used to determine the level of asymmetric environment around Ln<sup>3+</sup> and covalency between Ln<sup>3+</sup> and neighbour particle [3,10]. The  $\Omega_4$  and  $\Omega_6$  show the viscosity and rigidity level of glass host [1,3,10]. The JO parameters of glass show the trend of  $\Omega_2 > \Omega_4 > \Omega_6$ . From overall value of  $f_{exp}$ ,  $f_{cal}$  and  $\Omega_\lambda$ , the thermal correction enhances these values to be higher than

ones without thermal correction. Obtained  $\Omega_2$ ,  $\Omega_4$  and  $\Omega_6$  are used to evaluated the radiative parameters from the emission spectra consisting of radiative transition possibility ( $A_R$ ), stimulated emission cross-section ( $\sigma$ ) and branching ratio ( $\beta_R$ ) for with and without thermal correction as shown in table 2. The  ${}^5\text{D}_0 \rightarrow {}^7\text{F}_2$  transitions (613 nm emission) performs the highest value of  $A_R$ ,  $\sigma$  and  $\beta_R$ . The highest  $A_R$  represents the highest transition probability of  $\text{Eu}^{3+}$  from  ${}^5\text{D}_0$  to  ${}^7\text{F}_2$ , corresponding with the intensity in spectrum. The largest  $\sigma$  show that  ${}^5\text{D}_0 \rightarrow {}^7\text{F}_2$  transition use the lowest threshold energy for the laser generation and release the highest laser gain application [3,10,14], compared

with other transitions in this glass. The highest  $\beta$  value with higher than 0.50 performs the highest lasing power produced form  ${}^5\text{D}_0 \rightarrow {}^7\text{F}_2$  transition. The  $\beta_R$  values are compared with  $\beta_{\text{exp}}$  evaluated form the integrated intensity of each emission peak [3]. The difference of  $\beta_R$  and  $\beta_{\text{exp}}$  value for some transitions comes from the mathematical deviation of Judd-Ofelt analysis. From overall value of radiative parameters, the thermal correction enhances these values to be higher than ones without thermal correction. J-O analysis indicates that CaGdSiBFEu glass performs a good potential for using as laser medium with 613 nm emission under  ${}^5\text{D}_0 \rightarrow {}^7\text{F}_2$  transition of  $\text{Eu}^{3+}$ .

**Table 1.** Transition, wavenumber ( $\nu$ ,  $\text{cm}^{-1}$ ), experimental ( $f_{\text{exp}}$ ) and calculated ( $f_{\text{cal}}$ ) oscillator strengths ( $\times 10^{-6}$ ), and the Judd-Ofelt parameters  $\Omega_\lambda$  ( $\lambda= 2, 4$  and  $6$ ) ( $\times 10^{-20}$   $\text{cm}^2$ ) without and with thermal correction of the 1.0 mol%  $\text{Eu}^{3+}$  ion doped glass.

Transition	$\nu$	Oscillator strengths			
		Without thermal Correction		With thermal correction	
		$f_{\text{exp}}$	$f_{\text{cal}}$	$f_{\text{exp}}$	$f_{\text{cal}}$
${}^7\text{F}_0 \rightarrow {}^5\text{D}_4$	27624	0.611	0.499	1.018	1.010
${}^7\text{F}_0 \rightarrow {}^5\text{G}_5$	26810	0.211	0.000	0.352	0.000
${}^7\text{F}_0 \rightarrow {}^5\text{G}_3$	26596	0.041	0.000	0.068	0.000
${}^7\text{F}_0 \rightarrow {}^5\text{L}_6$	25381	2.367	1.277	3.945	3.019
${}^7\text{F}_1 \rightarrow {}^5\text{D}_3$	24213	0.201	0.214	0.503	0.457
${}^7\text{F}_0 \rightarrow {}^5\text{D}_2$	21505	0.268	0.293	0.447	0.721
${}^7\text{F}_0 \rightarrow {}^5\text{D}_1$	19011	0.042	0.000	0.070	0.000
${}^7\text{F}_1 \rightarrow {}^5\text{D}_1$	18832	0.281	0.278	0.703	0.684
${}^7\text{F}_0 \rightarrow {}^7\text{F}_6$	4766	2.789	2.243	4.648	5.304
${}^7\text{F}_1 \rightarrow {}^7\text{F}_6$	4543	1.785	1.854	4.463	4.385
rms		$\pm 0.410$		$\pm 0.401$	
$\Omega_2$		10.41		25.66	
$\Omega_4$		10.05		20.34	
$\Omega_6$		1.99		4.70	

**Table 2.** Emission band positions ( $\lambda_p$ , nm), radiative transition probabilities ( $A_R$ ,  $\text{s}^{-1}$ ), peak stimulated emission cross-sections ( $\sigma(\lambda_p)$ ,  $\times 10^{-22} \text{cm}^2$ ), and experimental and calculated branching ratios ( $\beta_R$ ) for  ${}^5\text{D}_0 \rightarrow {}^7\text{F}_J$  ( $J = 1, 2, 3$  and  $4$ ) transitions without and with thermal correction of the 1.0 mol%  $\text{Eu}^{3+}$  ion doped glass.

${}^5\text{D}_0 \rightarrow$	$\lambda_p$	Without thermal Correction				With thermal correction			
		$A_R$	$\sigma(\lambda_p)$	$\beta_R$		$A_R$	$\sigma(\lambda_p)$	$\beta_R$	
				$\beta_{R\_Exp}$	$\beta_{R\_Cal}$			$\beta_{R\_Exp}$	$\beta_{R\_Cal}$
${}^7\text{F}_0$	579	0.00	0.00	0.03	0.00	0.00	0.00	0.00	0.03
${}^7\text{F}_1$	590	64.30	2.38	0.21	0.09	64.30	2.38	0.19	0.21
${}^7\text{F}_2$	613	438.40	19.63	0.62	0.61	1080.40	48.37	0.68	0.62
${}^7\text{F}_3$	652	0.00	0.00	0.03	0.00	0.00	0.00	0.04	0.00
${}^7\text{F}_4$	701	211.90	14.98	0.09	0.30	428.80	30.31	0.09	0.27

The indirect and direct band gap energy of glass are evaluated in figure 5 as 2.795 and 3.242 eV, respectively. Figure 6 shows the FTIR spectrum of the CaGdSiBFEu glass. The strong infrared absorption band at  $1165\text{ cm}^{-1}$  originates from the vibration of  $\text{BO}_3$  and  $\text{BO}_4$  with tri-, tetra-, pentaborate and diborate unit structure, along with the asymmetric stretching of Si-O-Si bonds [15,16]. The CIE 1931 chromaticity diagram was used to analyze color of emission, which indicate the chromaticity visible to the human eye. The emission spectrum with 275 excitation wavelength of the CaGdSiBFEu glass was selected to monitor the color of emitted light. The CIE color coordinate ( $x$ ,  $y$ ) shows at (0.64, 0.36), which were plotted at the edge of reddish orange region in color diagram as shown in figure 7.

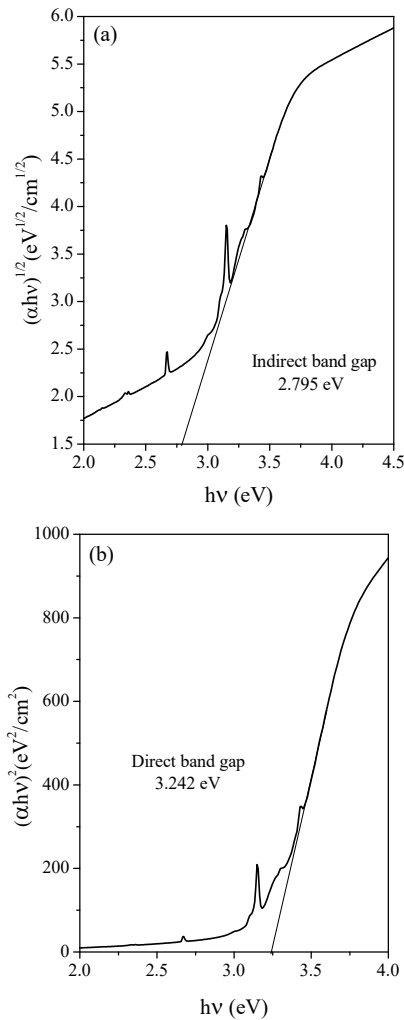


**Figure 5.** (a) Indirect band gap and (b) direct band gap of the CaGdSiBFEu glass.

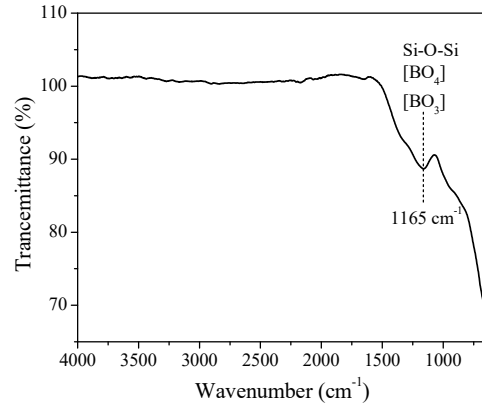


**Figure 6.** FTIR spectrum of the CaGdSiBFEu glass.

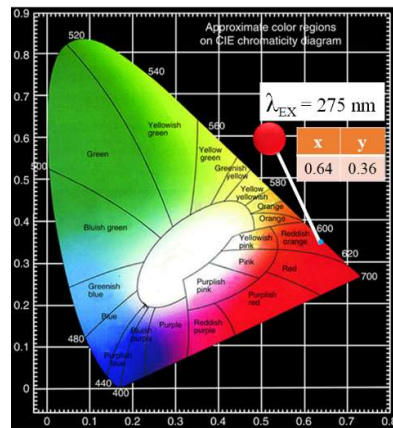


**Figure 7.** The CIE 1931 chromaticity diagram of the CaGdSiBFEu glass.

#### 4. Conclusions

The  $\text{Eu}^{3+}$  ion doped calcium gadolinium silicoborate oxyfluoride glass was prepared by melt-quenching technique. The results of glass absorbed photon in ultraviolet, visible light and near infrared regions. This glass shows the strongest emission with 613 nm ( ${}^5\text{D}_0 \rightarrow {}^7\text{F}_2$ ) when it was excited by 275 nm wavelength. The detailed and systematic analysis of optical intensities has been performed from absorption and emission spectrum using J-O theory. The thermal correction method can improve the J-O and radiative parameters in J-O analysis process. The  $\sigma(\lambda_p)$  and  $\beta_R$  values for the  ${}^5\text{D}_0 \rightarrow {}^7\text{F}_2$  transition revealed that CaGdSiBFEu glass could be used for the development of laser device with 613 nm emission. The indirect and direct band gap energy of glass are 2.795 and 3.242 eV, respectively. The color coordinates ( $x$ ,  $y$ ) of glass is located at the point (0.64, 0.36) in reddish orange region of CIE 1931 chromaticity diagram.

## 5. Acknowledgements

This work was supported by Thailand Research Fund (TRF) through the Royal Golden Jubilee (RGJ) Ph.D. Program (Grant No. PHD/0100/2559).

## References

- [1] P. Babu and C. K. Jayasankar, "Optical spectroscopy of  $\text{Eu}^{3+}$  ions in lithium borate and lithium fluoroborate glasses," *Physica B: Condensed Matter*, vol. 279, pp. 262-281, 2000.
- [2] J. Kaewkhao, N. Wantana, S. Kaewjaeng, S. Kothan, and H. J. Kim, "Luminescence characteristics of  $\text{Dy}^{3+}$  doped  $\text{Gd}_2\text{O}_3$ -CaO-SiO<sub>2</sub>-B<sub>2</sub>O<sub>3</sub> scintillating glasses," *Journal of rare earths*, vol. 34, pp. 583-589, 2016.
- [3] N. Vijaya and C. K. Jayasankar, "Structural and spectroscopic properties of  $\text{Eu}^{3+}$ -doped zinc fluorophosphate glasses," *Journal of Molecular Structure*, vol. 1036, pp. 42-50, 2012.
- [4] K. Marimuthu, R. T. Karunakaran, S. Surendra Babu, G. Muralidharan, S. Arumugam, and C. K. Jayasankar, "Structural and spectroscopic investigations on  $\text{Eu}^{3+}$ -doped alkali fluoroborate glasses," *Solid State Sciences*, vol. 11, pp. 1297-1302, 2009.
- [5] K. Varshneya Arun, *Fundamentals of Inorganic Glasses*. United Kingdom: Academic Press Limited, 1994.
- [6] A. Antuzevics, M. Kemere, G. Kriek, and R. Ignatans, "Electron paramagnetic resonance and photoluminescence investigation of europium local structure in oxyfluoride glass ceramics containing  $\text{SrF}_2$  nanocrystals," *Optical Materials*, vol. 72, pp. 749-755, 2017.
- [7] G. Kriek, A. Sarakovskis, and M. Springis "Ordering of fluorite-type phases in erbium-doped oxyfluoride glass ceramics," *Journal of the European Ceramic Society*, vol. 38, pp. 235-243, 2018.
- [8] N. Mahendru, R. Bagga, K. Sharma, G. P. Kothiyal, M. Falconieri, and G. Sharma, "On the influence of lead and cadmium fluoride content on thermal, optical and structural properties of oxyfluoride glass," *Journal of Alloys and Compounds*, vol. 608, pp. 60-65, 2014.
- [9] N. Wantana, S. Kaewjaeng, S. Kothan, H. J. Kim, and J. Kaewkhao, "Energy transfer from  $\text{Gd}^{3+}$  to  $\text{Sm}^{3+}$  and luminescence characteristics of CaO-Gd<sub>2</sub>O<sub>3</sub>-SiO<sub>2</sub>-B<sub>2</sub>O<sub>3</sub> scintillating glasses," *Journal of Luminescence*, vol. 181, pp. 382-386, 2017.
- [10] E. Kaewnuam, N. Chanthima, C. K. Jayasankar, H. J. Kim, and J. Kaewkhao, "Optical, Luminescence and Judd-Oflet Study of  $\text{Eu}^{3+}$  Doped Lithium Yttrium Borate Glasses for Using as Laser Gain Medium," *Key Engineering Materials*, vol. 675-676, pp. 364-367, 2016.
- [11] P. Babu, K. H. Jang, E. S. Kim, R. Vijaya, C. K. Jayasankar, V. Lavín, and H. J. Seo, "Local field dependent fluorescence properties of  $\text{Eu}^{3+}$  ions in a fluorometaphosphate laser glass," *Journal of Non-Crystalline Solids*, vol. 357, pp. 2139-2147, 2011.
- [12] F. Xinjie, S. Lixin, and L. Jiacheng, "Radiation induced color centers in cerium-doped and cerium-free multicomponent silicate glasses," *Journal of Rare Earths*, vol. 32, pp. 1037-1042, 2014.
- [13] M. Farouk, A. Abd El-Maboud, M. Ibrahim, A. Ratep, and I. Kashif, "Optical properties of Lead bismuth borate glasses doped with neodymium oxide," *Spectrochimica Acta Part A: Molecular and Biomolecular*, vol. 149, pp. 338-342, 2015.
- [14] C. R. Kesavulu, K. K. Kumar, N. Vijaya, K. S. Lim, and C. K. Jayasankar, "Thermal, vibrational and optical properties of  $\text{Eu}^{3+}$ -doped lead fluorophosphate glasses for red laser applications," *Materials Chemistry and Physics*, vol. 141, pp. 903-911, 2013.
- [15] D. Singh, K. Singh, G. Singh, Manupriya, S. Mohan, M. Arora, and G. Sharma, "Optical and structural properties of ZnO-PbO-B<sub>2</sub>O<sub>3</sub> and ZnO-PbO-B<sub>2</sub>O<sub>3</sub>-SiO<sub>2</sub> glasses," *Journal of Physics: Condensed Matter*, vol. 20, pp. 1-6, 2008.
- [16] G. Shao, X. Wu, Y. Kong, X. Shen, S. Cui, X. Guan, C. Jiao, and J. Jiao, "Microstructure, radiative property and thermal shock behavior of TaSi<sub>2</sub>-SiO<sub>2</sub>-borosilicate glass coating for fibrous ZrO<sub>2</sub> ceramic insulation," *Journal of Alloys and Compounds*, vol. 663, pp. 360-370, 2016.